Unified electronic charge transport model for organic solar cells

Seyyed Sadegh Mottaghian,[1] Matt Biesecker,[2] Khadijeh Bayat,[3] and Mahdi Farrokh Baroughi[1,a)]

[1]*Department of Electrical Engineering and Computer Science, Daktronics Engineering Hall, South Dakota State University, Brookings, South Dakota 57007, USA*
[2]*Department of Mathematics, South Dakota State University, Brookings, South Dakota 57007, USA*
[3]*Harvard School of Engineering and Applied Sciences, Pierce Hall, 29 Oxford Street, Cambridge, Massachusetts 02138, USA*

(Received 20 April 2013; accepted 18 June 2013; published online 8 July 2013)

This paper provides a comprehensive modeling approach for simulation of electronic charge transport in excitonic solar cells with organic and organic/inorganic structures. Interaction of energy carrying particles (electrons, holes, singlet excitons, and triplet excitons) with each other and their transformation in the bulk of the donor and acceptor media as well as the donor/acceptor interfaces are incorporated in form of coupling matrices into the continuity equations and interface boundary conditions. As a case study, the model is applied to simulate an organic bilayer photovoltaic (PV) device to quantify the effects of photo generation, recombination coefficient, carrier mobility, and electrode work function on its PV characteristics. The study proves that electron-hole recombination at the donor/acceptor interface is the dominant mechanism that limits open circuit voltage of the device. © *2013 AIP Publishing LLC*. [http://dx.doi.org/10.1063/1.4813099]

I. INTRODUCTION

Flexibility, easy processing, and the potential for low production cost of organic based light emitting diodes and solar cells have led to intensive studies on the development and utilization of conjugated polymers, organic dyes, and organic-inorganic hybrids for photovoltaic device (PV) applications.[1,2] Unlike the charge transport in inorganic semiconductors and devices, transport of energy carrying particles which include electrons, holes and excitons in organic materials and organic-organic interfaces are not fully understood. Organic devices require comprehensive electronic/excitonic transport models to enhance our understanding of the physical processes occurring inside the PV devices.

Deterministic approaches based on partial differential equations (PDE) derived from particle conservation (continuity) laws and Poisson and flux equations can be utilized to analyze complex electronic systems incorporating interactions of multiple types of energy-carrying particles. Drift-diffusion equations with some modification on the mobility and diffusion coefficient models, derived from the conservations laws[3] accompanied by Poisson and flux equations, can be used to model organic PV materials and devices.[4–13] This provides a basis to unify charge transport models in organic and inorganic material and device systems. Koster *et al.*[10] applied this model to simulate electron/hole/exciton transport in the bulk heterojunction solar cells assuming an effective single absorber/transport layer with metal-insulator-metal (MIM) structure.

Two dimensional modeling of organic solar cells have been reported by Martin *et al.*[14,15] to simulate nanoscale charge transport in ordered bulk heterojunction solar cells. However, their model considered only transport of electrons in acceptor and holes in donor and disregard bipolar charge transport in the bulk of a solar cell. Kirchartz *et al.*[9] reduced the two dimensional bulk heterojunction geometry into a MIM structure and solved the charge transport equations in an effective donor/acceptor medium. Most of the aforementioned works used a MIM device structure, assuming the entire donor/acceptor blend as a single light absorber and charge transport layer. This prevents in depth understanding of donor/acceptor interfaces despite their significance for the performance of PV devices and also prevents independent assessment of donor and acceptor properties on the photovoltaic performance of organic solar cells. Cuiffi *et al.* have solved the coupled Poisson and electron/hole continuity equations in an organic bilayer device. They considered exciton dissociation as a free electron hole generation rate at the donor-acceptor interface without explicitly solving the exciton continuity equation.[16]

Based on this review, there is a need for developing a comprehensive model for transport and coupling of energy carrying particles in the bulk and interfaces of organic and organic/inorganic material systems. This article presents a general charge transport model for organic, inorganic, and hybrid photoactive electronic devices.

II. MODEL DESCRIPTION

A. Unified charge transport model

Modeling of charge transport in nanostructured PV devices requires rigorous mathematical transport models for the description of electron/hole transport in the bulk of both organic and inorganic materials, exciton (singlet or triplet) transportation in the bulk of organic materials, and possible interactions of energy-carrying particles with the interface states in nanostructured heterointerfaces. Here, we present a unified transport model for transport of electrons, holes,

a)Author to whom correspondence should be addressed. Electronic mail: m.farrokhbaroughi@sdstate.edu. Tel.: 605-688-6963.

singlet excitons, and triplet excitons and the possible interactions in the bulk of the donor and acceptor regions as well as the donor/acceptor interfaces. The model can be utilized to simulate photovoltaic properties of variety of organic and organic/inorganic solar cells.

Figure 1 shows the various energy-carrying particles in the generalized organic-inorganic electronic system with possible transformation of each particle into another through a transformation rate constant (k). The parameters $k_{\mathrm{np,T}}$, $k_{\mathrm{X,np}}$, $k_{\mathrm{T,np}}$, $k_{\mathrm{T,np}}$, $k_{\mathrm{X,T}}$, and $k_{\mathrm{T,X}}$ terms, represent the coupling of the various energy carrying particles in the bulk of semiconductors. In particular, $k_{\mathrm{x,y}}$ represents the transformation rate from particle "x" into particle "y." For example, $k_{\mathrm{np,X}}$ represent the transformation rate of free electron-hole pairs into singlet exciton.

The proposed unified charge transport model is given in the equation set (1)–(7). Equation (1) is Poisson's equation relating the density of electric charges (electrons n, holes p, ionized donor $\mathrm{N_D}^+$ and acceptor $\mathrm{N_A}^-$ dopant particles, trapped electrons n_{T} and holes p_{T}) to the electronic potential (ψ).[7,8,10] Equations (2)–(5) represent the continuity equations[10,17] for electrons (n), holes (p), singlet excitons (X), and triplets excitons (T), respectively. Each energy carrier particle can be generated by electrical injection through contacts, and thermal or optical excitation. These particles can travel through diffusion, drift, or drift-diffusion mechanisms throughout the material, transform to another energy carrying particle or vanish through recombination process. G_{x} represents the generation rate of particle "x" and R_{np}, R_{X}, and R_{T} represent the recombination rates for electrons-holes, singlet, and triplet excitons, respectively. The elements C_{np}, C_{X}, and C_{T} in Eqs. (2)–(5) originate from cross coupling of energy carrying particles according to Eq. (6)

$$\nabla^2\psi = \frac{q}{\varepsilon}(p - n + N_D{}^+ - N_A{}^- + p_T - n_T), \tag{1}$$

$$\partial n/\partial t = D_n\nabla^2 n + \mu_n\nabla n\nabla\psi + \mu_n n\nabla^2\psi + G_{op,n} - R_{np} + C_{np}, \tag{2}$$

$$\partial p/\partial t = D_p\nabla^2 p - \mu_p\nabla p\nabla\psi - \mu_p p\nabla^2\psi + G_{op,p} - R_{np} + C_{np}, \tag{3}$$

$$\partial X/\partial t = D_X\nabla^2 X + G_{op,X} - R_X + C_X, \tag{4}$$

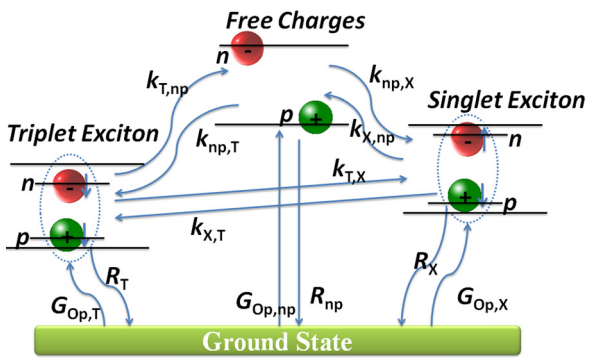

FIG. 1. A generalized electronic model for organic and inorganic material systems with free electrons, holes, singlet excitons, and triplet excitons as the energy carrying particles.

$$\partial T/\partial t = D_T\nabla^2 T + G_{op,T} - R_T + C_T, \tag{5}$$

where $G_{Op,n}$ and $G_{Op,p}$ contain the $G_{Op,np}$ and electron and hole generation from exciton dissociation which is described in supplementary material.[18] The coupling quantities (C_{np}, C_{X}, and C_{T}) are given by

$$\begin{bmatrix} C_{np} \\ C_X \\ C_T \end{bmatrix} = \begin{bmatrix} -k_{np,X} - k_{np,T} & k_{X,np} & k_{T,np} \\ k_{np,X} & -k_{X,np} - k_{X,T} & k_{T,X} \\ k_{np,T} & k_{X,T} & -k_{T,np} - k_{T,X} \end{bmatrix} \begin{bmatrix} np \\ X \\ T \end{bmatrix}, \tag{6}$$

where μ_{n} and μ_{p} in Eqs. (2) and (3) represent the field and concentration dependent mobility of electrons and holes, respectively. The constants D_{n}, D_{p}, D_{X} and D_{T} are the diffusion coefficients for electrons, holes, singlet excitons, and triplet excitons. The transformation rates also can depends on electric field and the density of the various energy carrying particles. In a comprehensive organic semiconductor domain, the coupled equation set of (1)–(6) have to be solved concurrently. In an inorganic domain, only Eqs. (1)–(3) have to be solved simultaneously, whereas in a hybrid organic/inorganic system, Eqs. (1)–(3) apply to both domains and Eqs. (4)–(6) apply only to the organic domain. The boundary conditions at the organic/inorganic interfaces would couple the equations in the organic medium to those of inorganic medium.

The recombination of free carriers in Eqs. (2) and (3) represented by R_{np} is often the dominant recombination mechanism in the semiconductor material. Three components that give rise to R_{np} are the band to band recombination (direct band recombination in inorganic semiconductor and Langevin bimolecular recombination in organic semiconductors), trap-assisted Shockley–Read–Hall (SRH) recombination (inorganic and organic semiconductors), and band to band Auger recombination (inorganic and organic semiconductors). Hence, R_{np} in general can be given by[19]

$$R_{np} = \beta(np - n_i^2) + \int_{E_{\min}}^{E_{\max}} \frac{np - n_i^2}{(n+n_1)/(\sigma_p v_{t,p}) + (p+p_1)/(\sigma_n v_{t,n})} \times N_T(E_T)dE_T + [c_n(n^2p - n_0^2p_0) + c_p(p^2n - p_0^2n_0)], \tag{7}$$

where n_{i} is the density of free carriers in an intrinsic semiconductor, n_0 and p_0 are density of electrons and holes in the semiconductor under thermal equilibrium, $n_1 = n_{\mathrm{i}}\exp[(E_{\mathrm{T}} - E_{\mathrm{i}})/kT]$ and $p_1 = n_{\mathrm{i}}$. Also, E_{T} and $N_{\mathrm{T}}(E_{\mathrm{T}})$ are the energy of the trap level and distribution of the dominant trap states throughout the bandgap, σ_{n} and σ_{p} are the capture cross section of trap states for the electron and hole capture processes, $v_{\mathrm{t,n}}$ and $v_{\mathrm{t,p}}$ are the thermal velocity values associated with electrons and holes, and c_{n} and c_{p} are the coefficients associated with the Auger recombination mechanism.

B. Interfacial processes for excitons and interface boundary conditions

Exciton dissociation (relaxation at large band-offset heterointerfaces) and recombination (through charge transfer

centers) are two major excitonic interfacial processes. Another possible interfacial exciton transport phenomenon is injection of excitons from one organic medium to another through the Förster and Dexter resonance energy transfer processes. Unifying the possible interfacial processes through an exciton conservation principle into a complete interface boundary condition leads to the system of equations

$$\begin{bmatrix} -D_1 \nabla X_1 \bullet \hat{S}_1 \\ -D_2 \nabla X_2 \bullet \hat{S}_2 \end{bmatrix} = \begin{bmatrix} K_{r1} + K_{i1} + K_{d1} & -K_{i2} \\ -K_{i1} & K_{r2} + K_{i2} + K_{d2} \end{bmatrix} \begin{bmatrix} X_1 \\ X_2 \end{bmatrix}, \tag{8}$$

where k_d, k_r, and k_i are the rate constants associated with the interfacial exciton dissociation, interfacial exciton recombination, and exciton injection processes. X_1 and X_2 represent density of singlet excitons at the neighboring mesh points of the interface, while S_1 and S_2 represent the unit normal vector to media one and two. The left hand side of Eq. (8) is the flux of singlet excitons at the interface from donor and acceptor media. The right hand side encapsulates the recombination, injection, and dissociation processes for singlet excitons. These two boundary conditions couple the continuity equations for excitons in donor and acceptor media. As a result of this formulation, the flux of dissociated singlet excitons (J_{Xd}) at the donor/acceptor interface can be given by

$$J_{Xd} = k_d X_1 + k_d X_2. \tag{9}$$

As proposed by Bredas,[20] the exciton dissociation at an appropriate donor/acceptor interface happens through formation and dissociation of the charge transfer centers(CTC). If the electron and hole pair remain in a CTC state and lose their kinetic energies, it is highly possible that they would recombine. As a result, it can be perceived that dissociated electrons and holes do not form right at the interface but within a small distance from the interface.[21] We propose $f_n(r)$ and $f_p(r)$ functions with β-distribution (with α and β parameters of 2 and 5, respectively), to represent the distribution of electron an hole generation rates in the vicinity of the interface, due to exciton dissociation inside the acceptor and donor media, respectively. The distance between the maxima of $f_n(r)$ and $f_p(r)$ is 2nm. This is helpful because using a smooth generation function instead of a delta function, improves the numerical stability of the PDE solver. It should be noted that the dimension of $f_n(r)$ and $f_p(r)$ is cm^{-1} and the one dimensional integral of $f_n(r)$ and $f_p(r)$ at the vicinity (often within 2 nm) of the interface is unity. Based on this concept, the electron and hole generation functions due to exciton dissociation can be formulated as

$$G_{in}(r) = (k_{d1}X_1 + k_{d2}X_2) f_n(r - r_I), \tag{10a}$$

$$G_{ip}(r) = (k_{d1}X_1 + k_{d2}X_2) f_p(r - r_I), \tag{10b}$$

where r_I represents the closest point at the donor/acceptor interface to the point r. The terms $G_{in}(r)$ and $G_{ip}(r)$ are the electron and hole generation rates due to exciton dissociation in the vicinity of the interface. Observed that $G_{in}(r)$ and $G_{ip}(r)$ are added to the optical generation rates of electrons and holes, $G_{Op,np}(r)$, to give the total electron and hole generations rates of $G_{op,n}(r)$ and $G_{op,p}(r)$ in the continuity Eqs. (2) and (3)

$$G_{op,n}(r) = G_{op,np}(r) + G_{in}(r), \tag{10c}$$

$$G_{op,p}(r) = G_{op,np}(r) + G_{ip}(r). \tag{10d}$$

The formulation here is general and also applies to triplet excitons through replacing the density, the rate constants, and diffusion coefficient of singlet excitons by those of the triplet excitons. It should be noted that in material systems with slow rate of intersystem crossing, similar to the case of polythiophene (1 ns^{-1}),[22] the density and then the transport of triplet excitons can be ignored.

III. CASE STUDY ON A BILAYER ORGANIC SOLAR CELL

A bilayer organic photovoltaic device is being selected as the sample solar cell to verify the validity of the charge transport model. This enables us to validate the proposed model with no simplifying assumption on a device structure, where significant experimental results exist. This would quantitatively address the effect of various material parameters on the illuminated current-voltage (IV) characteristic of the bilayer organic PV device. Although this study is being implemented on a 1D bilayer device, this comprehensive approach can be easily expanded into bulk-heterojunction organic solar cells using an effective medium approximation.

The result of this simulation were obtained by numerical solution of the proposed model by a combination of Gummel and Newton methods, on a planar bilayer organic device (Fig. 2), with P3HT and PCBM as the donor and the acceptor media.[18] The parameters associated with the unified charge transport model, extracted from experimental results are listed the supplementary material.[18] The device simulated using the parameters listed in the table is considered as the baseline for the comparison. The spectral photon flux of AM 1.5 is used as the input illumination spectrum [$\varphi_i(\lambda)$] in all of the simulations. Spectral absorption coefficients for P3HT and PCBM are adopted from literature.[23,24] Due to small density of holes in acceptor and electrons in the donor media, the term $K_{np,X}$, which represents collapse of electron-hole

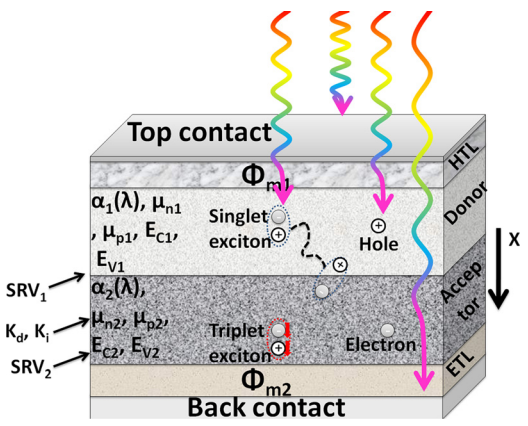

FIG. 2. (a) Structure of the organic solar cell for a case study with a 100 nm layer of P3HT and a 100 nm of PCBM.

pairs into a singlet exciton state, is negligible. At room temperature the term $K_{X,np}$ is also negligible due to much larger binding energies of excitons when compared to that of thermal energy. Therefore, the exciton transport equation was independently solved in the device structure of Fig. 2.

Figures 3(a) and 3(b) show the energy band structure of the baseline device under AM1.5 illumination for short circuit and open circuit conditions, respectively. Due to the negligible doping density of the donor and acceptor medium, the electric potential throughout the band structure has a linear distribution suggesting that the electric field throughout the solar cell, except near the contacts, is almost constant under short circuit condition. Under open circuit conditions the potential distribution is constant and electric field inside the device is negligible.

The large band-offsets in the LUMO (1 eV) and HOMO (0.9 eV) levels significantly suppress back diffusion of electrons from the acceptor to the donor regions and holes from the donor to the acceptor regions. Meanwhile, the electric field favors transport of the free electrons and holes into their respective contacts. This significantly reduces the recombination loss rate in the bulk of the absorber layers, which is proportional to $(n \times p\text{-}n_i^2)$.

Figures 3(c) and 3(d) depicts the density of electrons and holes under short and open circuit conditions, respectively. Density of excitons, which is independent of electric bias condition, is shown in Fig. 3(c). Even though the acceptor and donor media are undoped, they both exhibit doped semiconductor behavior. This is due to the fact that the photogenerated electrons, through exciton dissociation, are selectively injected into the acceptor medium, whereas photogenerated holes are injected to the donor medium. The injected electrons and holes change their respective quasi-Fermi levels. This is completely different than the case of inorganic PV materials where photogeneration in an absorber leads to generation of an electron and a hole in the same medium.

From the charge transport perspective, three regions can be identified: (i) bulk of the donor and acceptor (regions B and D), (ii) neighborhood of the donor/acceptor interface (region C), and (iii) neighborhood of the contacts (regions A and E). The current flow in the B and D regions is mainly dominated by the drift mechanism because the distribution of electrons and holes along with the electric field (slope of the LUMO or HOMO levels) in these regions are approximately constant. Charge conservation yields equal electric current at any given cross-section of the device (including donor and acceptor regions). Consequently, the density of free carriers in the low mobility side (holes in P3HT) will be higher than density of carriers in the high mobility side (electrons in PCBM). This is consistent with the results obtained from MIM models.[13]

Electron hole recombination is relatively large in vicinity of the donor/acceptor interface (region C) where $(n \times p - n_i^2)$ is much larger than in the bulk regions [Fig. 3(d)]. The much higher density of electrons in region "E" and holes in regions "A" compared to the bulk regions suggest that the charge transport is not contact limited and thus the simulation results reflect the physics of the bilayer device.

Flux of dissociated excitons at the donor/acceptor interface, J_{Xd}, depends on exciton dissociation rate, the absorption coefficient of the semiconductors, device thickness, device structure, exciton diffusion length, exciton lifetime, light intensity, and exciton surface recombination velocity. Therefore, dependence of the IV characteristics of the device on J_{Xd} represents collective effects of all the aforementioned material and device parameters. Figure 4(a) shows the current-voltage (IV) characteristic of the device, simulated for various fluxes of dissociated excitons. Increasing J_{Xd}

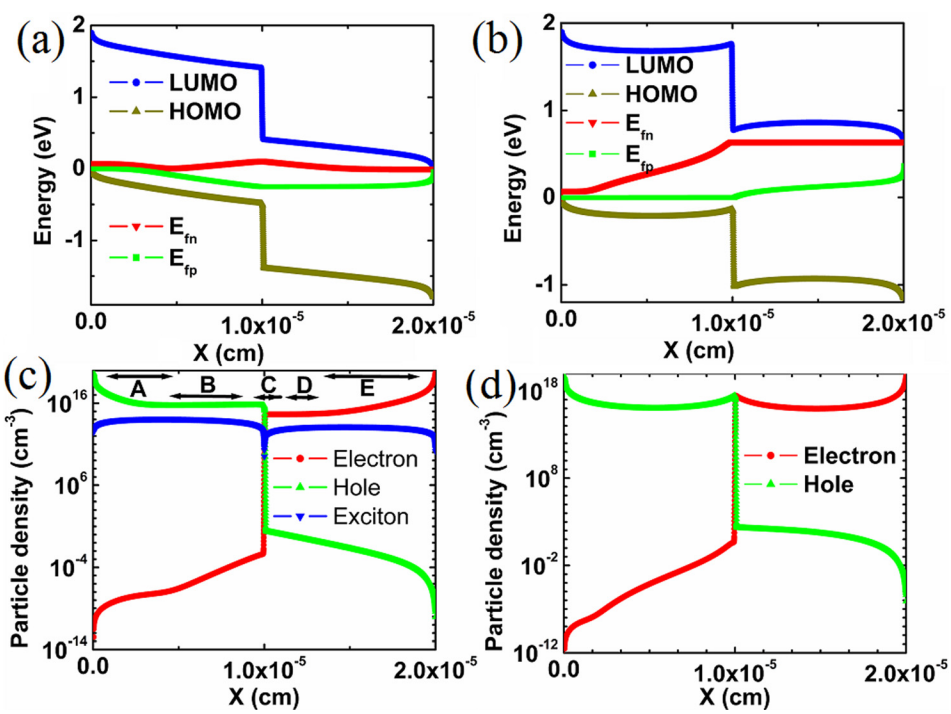

FIG. 3. Band diagram of the device under short (a) and open (b) circuit conditions both simulated under AM1.5 illumination where light is illuminated from left side. Density of electron (red), holes (green), and excitons (blue) in the device under short (c) and open (d) circuit conditions.

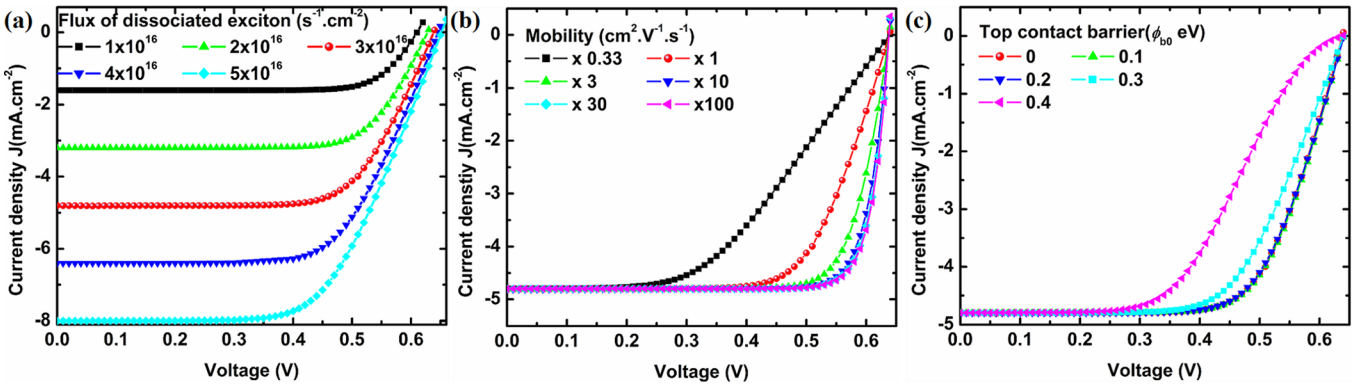

FIG. 4. IV characteristics of the bilayer organic solar cell considering (a) different flux of dissociated excitons (J_{Xd} in cm^{-2}/s), (b) different values of mobility. (Electron and hole mobility values in both donor and acceptor material scaled by the same factors of 1/3, 3, 10, 30, and 100), (c) different energy barriers at the top contact (difference between HOMO level of donor and work function of the front contact). The simulation was conducted under AM1.5 spectrum and ohmic back contact.

increases the density of electrons in acceptor and holes in the donor regions leading to larger difference in the quasi Fermi levels and the V_{OC} of the solar cell.[25,26] In this case study, the V_{OC} of the device is linearly dependent on $\log_{10}(J_{XD})$ with a rate of 60 mV/decade. Also J_{SC} shows a one to one linear dependence on J_{XD}.

Figure 4(b) shows the effect of electron and hole mobility values on the IV characteristics of the solar cell. The mobility values of P3HT and PCBM, are increased with the same ratio in multiplies of 3, 10, 30, and 100 respect to those of the baseline cell. Electron and hole mobility values affect the fill factor (FF) of the device significantly. Nevertheless, the IV characteristics lose its sensitivity to mobility of free carriers when they become larger than 10 times of the reference mobility values. This is consistent with prior experimental[27] and simulation results.[28] The results in Fig. 4(b) also suggest that the V_{OC} and J_{SC} of the solar cell is nearly independent of the free carrier mobility. The insensitivity of the J_{SC} to the free carrier mobility can be explained by the fact that the electron and hole extraction time is much shorter than the recombination time scale (mainly at the donor/acceptor interface) of free carriers for the simulated mobility regime. Also the fact that the mobility values do not affect the open circuit voltage for the studied regime indicates that the charge transport in this solar cell is dominated by recombination at the interface rather than the bulk of donor and acceptor regions. These might not be the case if the mobility values are much lower (multiple orders of magnitude) than the simulated values in this work. In such cases, mobility can affect J_{SC} and V_{OC} values.

Contacts to the donor and acceptor media also play an important role in the performance characteristics of solar cells. In all of the previous simulations, the work function of the front electrode was equal to the ionization potential of P3HT (donor) and the work function of the back contact was equal to the electron affinity of the PCBM (acceptor). This ensured achieving accumulation of majority-like carriers at the vicinity of contact and lead to ohmic contacts for transport of holes and electrons in the front and back contacts, respectively. In general, to achieve an ohmic contact to the donor (acceptor) medium the metal or transparent conductor is preferred to have a work function equal or larger (smaller) than ionization potential (electron affinity) of the donor (acceptor) medium. A mismatch between the work function of electrode and donor or acceptor medium can lead to a potential barrier detrimental to the performance characteristics of the solar cell. Such a barrier in the contact region can (i) reduce the density of charges near the contact (electrons in acceptor and holes in donor), therefore increase the series resistance of the solar cell and (ii) suppress the extraction of free carriers at the contact due to the formation of a reverse electric field at the vicinity of the contact region. Figure 4(c) shows the effect of the front contact work function on the illuminated IV characteristics of the bilayer organic solar cell. The value of ϕ_{b0} represents the difference in the HOMO level of P3HT and the work function of the front electrode. The back contact is ohmic in this simulation.

The IV characteristic of the solar cell is not sensitive to the ϕ_{b0} up to 0.2 eV mismatch. This includes negative values for ϕ_{b0} as well. In this regime, the band bending at the vicinity of the contact leads to accumulation of holes so the contact region has a much smaller resistivity than the bulk of the donor layer (similar to the results observed in Fig. 3(d)).

As a result, the contact is not a limiting factor in this regime. It should be noted that the difference in the quasi-Fermi level of holes and HOMO level of P3HT under light illumination, depicted in Fig. 3(b) is about 0.25 eV. The ϕ_{b0} values beyond 0.3 eV leads to a significantly reduced fill factor. Further increase in the value of ϕ_{b0}, 0.4 eV and higher changes the IV characteristic of the solar cell into an S-shape. S-shape behavior of illuminated IV have been repeatedly reported experimentally and has been qualitatively attributed to either work function of contacts or the mobility of free carriers.[6,29] Our study suggests that ϕ_{b0} at contacts must be kept smaller than 0.25 eV in order to avoid contact induced fill factor reduction.

Figure 5(a) shows the effect of direct recombination coefficient [β in Eq. (7)] in both acceptor and donor medium on the IV characteristic of the bilayer solar cell. The results indicate that an increase in the value of β shifts the IV characteristic towards lower voltages leading to reduced open circuit voltage proportional to $\log_{10}(\beta)$ with a rate of 59 mV/decade. Nevertheless, within the window of 4×10^{-10} to 10^{-7} cm^3/s, β appears to have no effect in the value of short

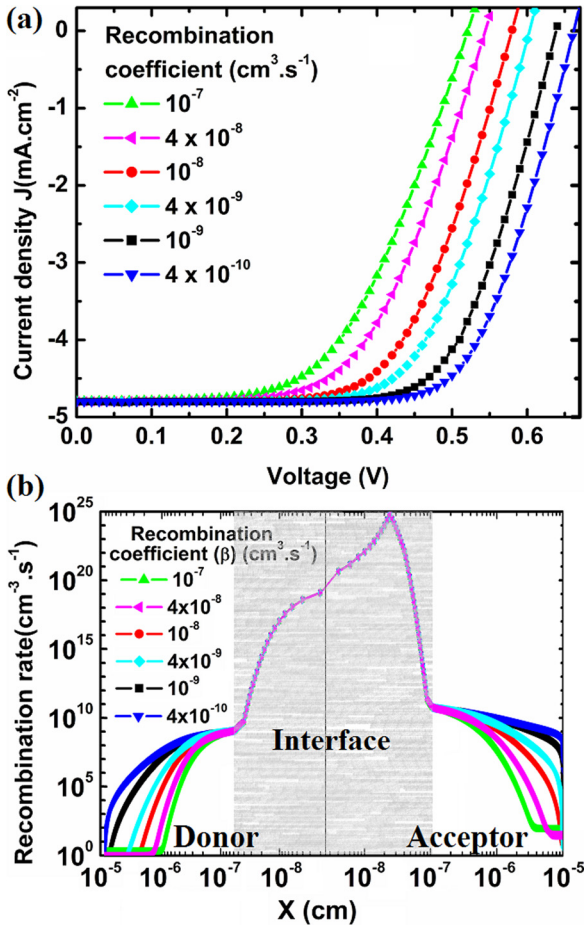

FIG. 5. (a) Effect of direct recombination coefficient in the bulk of both acceptor and donor media on the IV characteristics of the bilayer organic solar cell. (b) Recombination rate as a function of β throughout the bilayer organic solar cell under open circuit condition. The x-axis, in log-scale, shows the distance from the donor/acceptor interface.

circuit current nor on the overall shape of the illuminated IV characteristic. Figure 5(b) plots the recombination rate throughout the structure of the bilayer solar cell using donor/acceptor interface as the origin of this log-scale plot in both directions. The results show that almost all the recombination occurs in the neighborhood of the donor/acceptor interface, where the product of n and p is multiple orders of magnitude larger than in the bulk of acceptor and donor regions. This can be explained by the very low density of electrons in the donor and holes in the acceptor medium due to selective injection of electron and holes to the acceptor and donor media by exciton dissociation at the donor/acceptor interface. This is fundamentally different than in inorganic solar cells, where photogeneration in the absorber raises the density of both electrons and holes therefore recombination within the bulk becomes significant. The results of Fig. 5(b) also indicate the total recombination rate for all the studied values of β remains almost identical at the neighborhood of the interface. Since J_X is constant for all the cases, a smaller β value leads to larger population of electrons in acceptor and holes in the donor medium to keep βnp constant. This in turn leads to a larger quasi-Fermi levels separation and hence larger open circuit voltage. This is in compliance with the results illustrated in Fig. 5(a). This is

TABLE I. Sensitivity analysis conducted on the performance characteristics of the bilayer solar cell versus important material and device parameters. S_U^W represents sensitivity of parameter W versus parameter U and is calculated by $\frac{U}{W} \times \frac{dW}{dU}$.

Parameter (*Par*)	$S_{Par}^{V_{OC}}$	$S_{Par}^{I_{SC}}$	S_{Par}^{FF}	Efficiency
J_{Xd} (upper limit)	4.4%	99.91%	−24.69%	77.97%
J_{Xd} (lower limit)	4.35%	99.97%	−6.18%	96.21%
Recombination (lower limit)	− 4.21%	0%	−1.96%	−6.17%
Mobility (upper limit)	0.24%	0%	−0.02%	0.22%
Mobility (lower limit)	0%	0.20%	50.16%	49.87%
Barrier energy at the contact ϕ_{b0} (eV) (upper limit)	− 7. 85%	0.41%	−99.36%	−108.97%

another indication of the interface recombination limited charge transport in the bilayer organic solar cell. Interfacial recombination can be even more critical in the device performance of large junction area PV devices such as polymer bulk heterojunction[14] and dye sensitized solar cells,[30] which have 100–1000 times larger junction areas compared to planar devices.

Table I summarizes the sensitivity of the V_{OC}, FF, I_{SC}, and efficiency of the bilayer organic solar cell to the important material and device parameters in their upper and lower limits of the variation window. The results suggest that V_{OC} is sensitive to the contact work function, recombination coefficient, and the flux of dissociated excitons. I_{SC} is highly sensitive to the flux of dissociated excitons with almost one to one ratio whereas it is almost independent of the mobility of free carriers as well as the work function of the contact in the simulation regime. Fill factor is very sensitive to the work function of the electrode and mobility of free carriers in the lower limit regime. Based on this study, efficiency of the bilayer organic solar cell is highly dependent on the flux of dissociated excitons, work function of the contact, and mobility of electrons in acceptor and holes in donor media.

IV. CONCLUSION

This paper introduced a comprehensive charge transport model for simulation of organic and organic/inorganic hybrid excitonic solar cells. As a case study, the model was implemented to quantify the impact of various material and device parameters on performance characteristics of a bilayer organic solar cell. The major conclusions based on this case study follow: (1) the surprisingly low density of electrons in the donor and holes in the acceptor medium suppresses recombination of photocarriers in the bulk of donor and acceptor regions. (2) Recombination of photocarriers at donor/acceptor interface is an important physical process that dominates the charge transport and the value of open circuit voltage. (3) While undoped, the donor and acceptor media exhibit p-doped and n-doped behavior due to selective injection of electrons into acceptor and holes to the donor media under light illumination. This pushes electron and hole quas-Fermi levels within 0.25 eV from the respective LUMO and HOMO levels in acceptor and donor media. This sets an approximate limit of 0.3 eV for ϕ_b values for the electric contacts. The proposed unified charge transport model

can be further applied on variety of organic and organic/inorganic solar cells to quantify impact of various materials and geometric device parameters on the performance characteristics of the device.

ACKNOWLEDGMENTS

This material was based upon the research work supported by the National Science Foundation (NSF) Grant No. 1102356, NSF/EPSCoR Grant No. 0903804, and by the State of South Dakota. The authors would like to thank Dr. Brian Moore for the technical support and access to Supercomputing Facility at the South Dakota State University.

[1]T. Kawatsu, V. Coropceanu, A. Ye, and J. Bredas, J. Phys. Chem. **112**, 3429 (2008).
[2]F. Gao, L. W. Campbell, Y. Xie, R. Devanathan, A. J. Peurrung, and W. J. Weber, IEEE Trans. Nucl. Sci. **55**, 1079 (2008).
[3]T. Kirchartz, K. Seino, J. M. Wagner, U. Rau, and F. Bechstedt, J. Appl. Phys. **105**, 104511, (2009).
[4]A. Wagenpfahl, D. Rauh, m. Binder, C. Deibel, and V. Dyakonov, Phys. Rev. B **82**, 115306 (2010).
[5]W. Vervisch, S. Biondo, G. Rivière, D. Duché, L. Escoubas, P. Torchio, J. Simon, and J. Rouzo, Appl. Phys. Lett. **98**, 253306 (2011).
[6]A. Wagenpfahl and C. Deibel, Phys. Rev. B **77**, 165332 (2010).
[7]J. A. Barker, C. M. Ramsdale, and N. C. Greenham, Phys. Rev. B **67**, 075205 (2003).
[8]T. Kirchartz and U. Rau, Thin Solid Films **516**, 7144 (2008).
[9]T. Kirchartz, B. E. Pieters, K. Taretto, and U. Rau, J. Appl. Phys. **104**, 094513 (2008).
[10]L. J. A. Koster, E. C. P. Smits, V. D. Mihailetchi, and P. W. M. Blom, Phys Rev. B **72**, 085205 (2005).
[11]R. Hausermann, E. Knapp, M. Moos, N. A. Reinke, T. Flatz, and B. Ruhstaller, J. Appl. Phys. **106**, 104507 (2009).
[12]G. A. Buxton and N. Clarke, J. Model. Simul. Mater. Sci. Eng. **15**, 13 (2007).
[13]S. Lacic and O. Inganas, J. Appl. Phys. **97**, 124901 (2005).
[14]C. M. Martin, V. M. Burlakov, H. E. Assender, and D. A. R. Barkhouse, J. Appl. Phys. **102**, 104506 (2007).
[15]C. M. Martin, V. M. Burlakov, and H. E. Assender, Sol. Energy Mater. Sol. Cells **90**, 900 (2006).
[16]J. Cuiffi, T. Benanti, W. J. Nam, and S. Fonash, Appl. Phys. Lett. **96**, 143307 (2010).
[17]E. Knapp, R. Hausermann, H. U. Schwarzenbach, and B. Ruhstaller, J. Appl. Phys. **108**, 054504 (2010).
[18]See supplementary material as http://dx.doi.org/10.1063/1.4813099 for numerical method, boundary conditions, and material parameters.
[19]D. K. Shroder, *Semiconductor Material and Device Characterization* (Wiley, New Jersey, 2006).
[20]J. L. Bredas, R. R. Chance, and R. Silbey, J. Phys. Chem. **85**, 756 (1981).
[21]J. R. Tumbleston, D. H. Ko, E. T. Samulski, and R. Lopez, J. Appl. Phys. **108**, 084514 (2010).
[22]J. Guo, H. Ohkita, H. Benten, and S. Ito, J. Am. Chem. Soc. **132**, 6154 (2010).
[23]E. Lioudakis, A. Othonos, I. Alexandrou, and Y. Hayashi, J. Appl. Phys. **102**, 083104 (2007).
[24]H. Hoppe, N. S. Sariciftci, and D. Meissner, Mol. Cryst. Liq. Cryst. **385**, 113 (2002).
[25]R. C. I. MacKenzie, T. Kirchartz, G. F. A. Dibb, and J. Nelson, J. Phys. Chem. C **115**, 9806 (2011).
[26]R. A. Street and M. Schoendorf, Phys. Rev. B **81**, 205307 (2010).
[27]R. A. Street, S. Cowan, and A. J. Heeger, Phys. Rev. B **82**, 121301(R) (2010).
[28]W. Tress, A. Petrich, M. Hummert, M. Hein, K. Leo, and M. Riede, Appl. Phys. Lett. **98**, 063301 (2011).
[29]A. M. Ballantyne, L. Chen, J. Dane, T. Hammant, F. M. Braun, M. Heeney, W. Duffy, I. McCulloch, D. D. C. Bradley, and J. Nelson, J. Adv. Funct. Mater. **18**, 2373 (2008).
[30]J. Nepal, S. S. Mottaghian, M. Biesecker, and M. F. Baroughi, Appl. Phys. Lett. **102**, 203503 (2013).